International Journal of Automation, Control and Intelligent Systems
Vol. 4, No. 1, 2018, pp. 1-11
http://www.aiscience.org/journal/ijacis
ISSN: 2381-7526 (Print); ISSN: 2381-7534 (Online)

Assistive Control of a Complaint Robot with Integrated Pneumatic Pump

Chen Wang, Henning Stoeppler*, Oleg Ivlev

Friedrich-Wilhelm-Bessel-Institute Research Company, Bremen, Germany

Abstract

Pneumatic actuated rehabilitation robots are presently been developed worldwide because of their compliant behavior as a result of the following qualities they possess: natural compressibility of air, light weight and their high power to weight ratio. Hence the basic physical human-robot-interaction is given and can be further improved by using soft actuators with elastic chambers and assistive controllers. However, practical application and clinical deployment of pneumatic robots are limited due to the condition of a significant quantity of compressed air. Especially assistive acting robots with sophisticated control algorithms and high-dynamic servo valves often need a pneumatic line or large external supply. In this paper we propose a new assistive control algorithm, which can be implemented on microcontrollers, wherein the external compressed air supply is replaced by an integrated miniature pneumatic pump without a pressure tank and for the output, a simple proportional valve is utilized. As an application of this simplified control system, a mobile variant of a pneumatic elbow trainer with self-alignment has been constructed. The efficacy of the developed assistive control is demonstrated through experiments with healthy subjects.

Keywords

Soft Robotic, Rehabilitation, Assistive Control, Compact, Internal Air Supply

Received: June 21, 2017 / Accepted: February 6, 2018 / Published online: March 30, 2018

1. Introduction

Pneumatic actuators are seen as beneficial for rehabilitation robots, because the inherent compliance of air is a natural advantage for a rudimentary human-robot-interaction. The high power to weight ratio assures a sufficient support for patients meanwhile the pneumatic robots have light weights and less inertias. But because of the non-linear behavior in both force and airflow dynamics, the control of pneumatic robots is always complex and difficult. Force and position sensors are required for most developed pneumatic robots, which causes an increase in the cost of these robots. Another disadvantage for pneumatic robots is the external compressed air supply, which strongly reduces the mobility of the robots and leads to an increase in their sizes. These disadvantages limit the clinical deployment and the home use for ambulatory users is almost impossible till date. Therefore, a compact, low cost pneumatic robot is needed, which provides assistive behavior and also can assure a safe human-robot-interaction.

Currently, numerous pneumatic actuated rehabilitation robots are been documented and a safe basic interaction between human and robot has been realized. Pneu-WREX is an evolution of its predecessor WREX [1] developed by University of California, it uses impedance control law combined with state estimation to achieve an adaptive assistance control [2]. The iPam developed by the University of Leeds based on two symmetric arms uses admittance and impedance control to ensure a safe and comfortable interaction between human and robot [3] [4]. The RUPERT uses open loop control and PID controller combined with Iterative Learning Control [5]. The Salford rehabilitation exoskeleton (SRE) is a multijoint gravity compensated upper

* Corresponding author
E-mail address: stoeppler@fwbi-bremen.de (H. Stoeppler)

arm assistive exoskeleton developed at the University of Salford [6] that supports three different control modes: joint position control, joint torque control and impedance control [7] [8]. All these mentioned robots need external compressed air supply and both position and force sensors. Except RUPERT, which uses three-way valves [9], all the other mentioned robots use servo valves for precise pressure control. The Figure 1(a) shows the block diagram of this mainstream control concept of pneumatic rehabilitation robots. The external compressed air supply with a pressure tank to compensate pressure fluctuations is necessary so far and both pressure and position sensors are essential for a safe assistive control. The same concept was also used in the assistive acting movement therapy devices with pneumatic soft actuators with rotary elastic chambers (REC-actuators), developed at the FWBI [10].

In this paper, a new assistive control algorithm is demonstrated, which does not require an exact pressure or force regulation. The concept block diagram is shown in Figure 1(b). A regulable pneumatic pump is used for the direct compressed air supply, instead of an external supply with a pressure tank and a proportional valve is used for the air outlet. This air supply system can be integrated into the device. The mobility of the device is therefore increased and the costs are reduced. No pressure or force sensor is needed for the control system, only position sensors are used. In order to realize assistive behavioral patterns, the predefined desired trajectory is no more static. It adapts to active human movements and when combined with simple PI controller, provides sufficient and assistive support for patients. This whole control system can be implemented on a microcontroller with a graphical user interface (GUI) on a touchscreen. This control system is tested on an elbow trainer as an exemplary application and the achievements of our previous work are also applied on this device. For example the shaftless soft bending joint based on pneumatic skewed rotary elastic chambers (sREC) and the position estimation based on flex sensors and artificial neural network (ANN), to compensate for corresponding hysteresis and nonlinearities [11]. The Figure 2 shows the finished prototype of the elbow trainer.

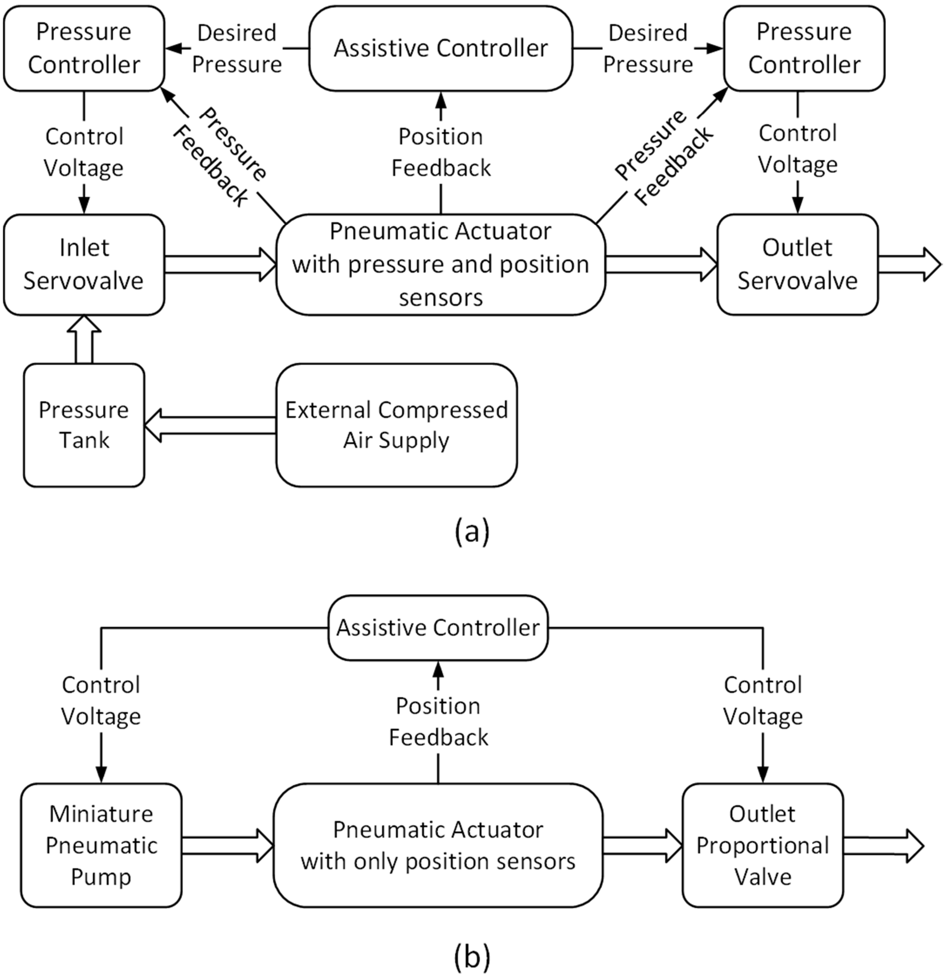

Figure 1. Assistive control conception of pneumatic rehabilitation robots: (a) scheme with externally compressed air supply and assistive control using pressure and position sensors; (b) simplified scheme with integrated pneumatic pump for directly compressed air.

Figure 2. Pneumatic elbow trainer: Prototype of a compact elbow trainer with integrated compressed air supply and assistive control system based on position sensors only. A touchscreen as control interface is used to make controlling more convenient.

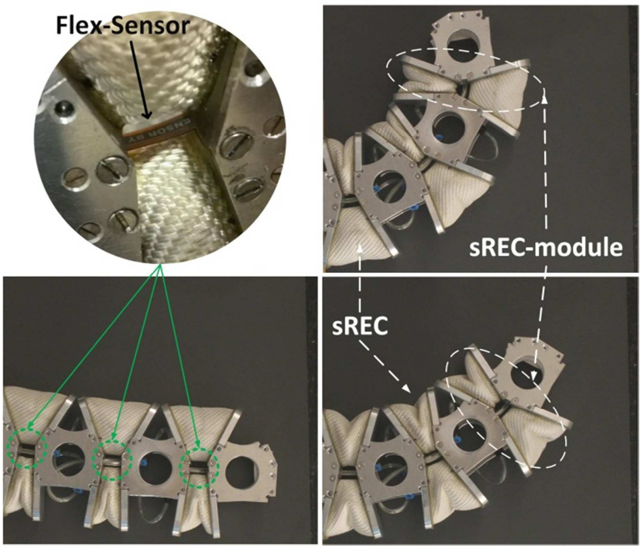

Figure 3. Pneumatic actuator: Structure of the sRECBA with three sREC-modules and an example of a motion sequence without an external load. In every sREC-module, a flex sensor is installed between the two sRECs.

2. Elbow Training Device

In comparison to the first prototype [11], which was only a laboratory setup, the base of this device is the frame and the pads with the straps from the commercial elbow trainer ARTROMOT E-2 (ORMED GmbH, Freiburg, Germany). This base, together with an integrated supply of air pressure and a microcontroller-based control unit, makes the new prototype compact and mobile. The kinematics of the robot is still the same as the first prototype.

2.1. Actuator

The basic elements that are used for actuator development are patented [12] self-made pneumatic bellows, the so called skewed Rotary Elastic Chambers (sREC) that provide a direct rotational motion without any mechanical rotation axis. To realize a bidirectional motion, two sRECs are mechanically connected antagonistically, resulting in a basic actuator element known as “sREC-module”. The stiffness of the actuator depends on the pressure provided in both actuator chambers. Finally, the actual realization of the sREC Bending Actuator (sRECBA) is built as a series of three of these actuator modules, see Figure 3. All bellows that work in the same direction are pneumatically connected to achieve a bidirectional rotary movement with an overall moving range of almost 120°. Due to the asymmetric arrangement of the bellows, the moving range of the actuator is adjusted to the moving range of human joints, providing hard stops at the moving range limits. Extensions to more than 0° (i.e. stretching) is mechanically restricted to ensure the safety of human joints such as the knee and/or elbow. As a result of the construction, sufficient actuator forces and torques can be achieved. For example, pressurized with 4 bar, the sRECBA can lift a load of up to 8 kg in the flexion direction. This force level is sufficient to support a movement of human joints such as the elbow or knee during rehabilitation. A more detailed description of the actuator is shown in [13].

2.2. Position Estimation

To determine the current position of the presented soft elbow trainer based on bending joint with implicit self-alignment, three less accurate but robust and cost-effective flex sensors are used as sensor systems. The flex sensors are the Spectra Symbol 2.5' flex sensor (Spectra Symbol, Salt Lake City, Utah, USA) and they are mounted in the middle of each sREC-module to measure the relative bending of the sREC-module.

The sensor system used for position estimation of the elbow trainer is shown in Figure 4. Flex sensors, also called resistive bending sensors, could offer an alternative for the position estimation of the shaftless soft actuators. Flex sensors are mainly used in sensor gloves or hand rehabilitation devices. The material composition of flex sensors with conducting layers has the effect of changing the resistance when the sensor becomes bended. The manufacturing of the flex sensors is simple and cheap, but the behavior and characteristic of the flex sensors are problematic, see Figure 4. ANN are used to compensate the corresponding nonlinearities and hysteresis effects.

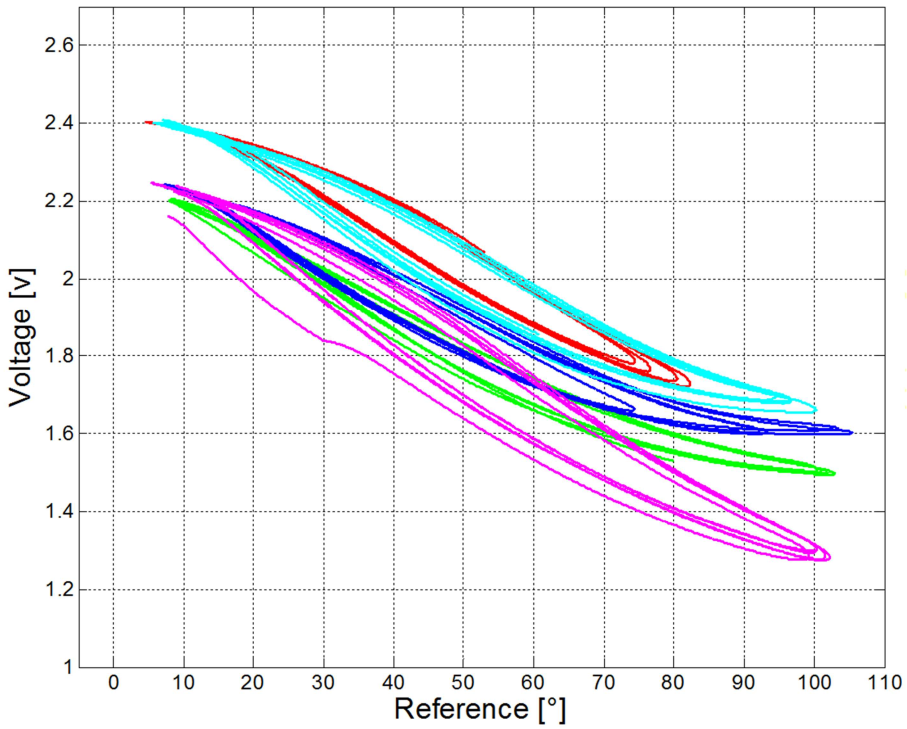

Figure 4. Characteristics of the voltage output of different flex sensors of the same type

The ANN for the position estimation are created with the Neural Network Toolbox as part of the software Matlab (The MathWorks Inc., Natick, Massachusetts, USA). The structure of the ANN is a single layer feed forward network with two inputs. The first is the sensor output voltage u_{flex}^T and to take the non-linearity and hysteresis effects into account, the derivative of the output voltage $\dot{u}_{flex}^T$ is used (see Eq. 1).

$$x_{ANN} = [u_{flex}^T \ \dot{u}_{flex}^T]^T \ \in \mathbb{R}^2. \tag{1}$$

The calculation of the flexion angle based on the ANN is defined as

$$\Phi_{ANN} = \sum_{K=1}^{n} O_K W_{\Omega,K} \tag{2}$$

with n as the number of hidden neurons, the weighting factor of the ANN is $W_{\Omega,K}$ and O_K is the output of the K^{th} hidden neuron

$$O_K = \tanh\left(\left(\sum_{\eta=1}^{2} x_{ANN} W_{K,\eta}\right) + \theta_K\right) \tag{3}$$

The training of the ANN was done by back propagation with the Levenberg-Marquardt optimization algorithm. The target value of the training data was the relative position between two inertial measurement units mounted on both sides of a sREC-module.

The proof of the successful compensation by the ANN could be seen in Figure 5.

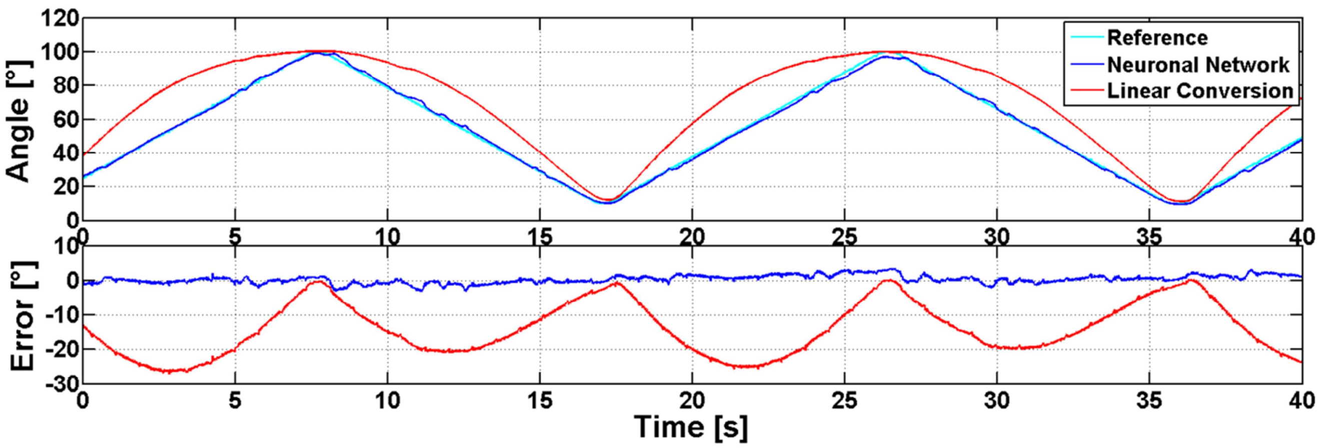

Figure 5. Result of the compensation of hysteresis and nonlinearities due to ANN on a test station.

2.3. Hardware Construction

For this new prototype, we have additionally built a control cabinet and control box, which can be seen in Figure 2. With the control cabinet and control box, the whole device is more compact and the mobility is increased. Furthermore, a convenient touch control is available on this device. The control cabinet consists of a control layer and a power supply layer. The Figure 6(a) shows the control layer. All the necessary control components, like pump, valve etc, are installed on this layer. The Figure 6(b) shows the power supply layer, which consists of the actual power supply units and the circuit breaker. In this work a miniature pump SP 622 EC-BL-DU-DV (Schwarzer Precision GmbH + Co. KG, Essen, Germany) has been used as a compressed air supply, which is shown in Figure 7(a) [14]. This pump offers two different connection ways. The parallel connection has a larger flow rate and a lower maximum pressure, which is 1.8 bar. The serial connection has a lower flow rate but a higher pressure, which can be more than 2.2 bar. The parallel connection is used in this work. As outlet valve a Kuhnke proportional valve type 68P (Kendrion GmbH, Industrial Control Systems, Malente, Germany) is used, which is shown in Figure 7(b) [15].

The value of the control voltages for the pump or valve are generated by the microcontroller, which can produce a maximum output of 3.3V. The pump and the valve both need 0-7 V and 0-24 V control voltage respectively. In order to drive the pump and valve correctly, the control voltage must be amplified first. Two amplifier circuits are used in the device. The amplifier circuit-A for the pump can amplify a voltage of 3.3V to 11V. The amplifier circuit-B amplifies the signal to a maximum of 22V. For the valve, we have to combine these both amplifier circuits to get the suitable control voltage. This means that the control voltage will be amplified through circuit-A and the output will be sent to circuit-B, where it will be further amplified to a maximum of 22V.

In the control box, the control core and a touch screen are installed. An Arduino Due board has been used for the control core (Arduino s.r.L., Turin, Italy), see Figure 8(a). This board has a 32-bit micro controller (AT91SAM3X8E), 512KB flash memory and 92 KB SRAM. The clock speed of the micro controller is 84 MHz. Altogether there are 12 analog pins and 54 digital pins available on the board. A 7 inch TFT LCD touch screen (SainSmart, Kansas, USA) is used to implement a simple touch control of the device. The control interface is shown in Figure 8(b).

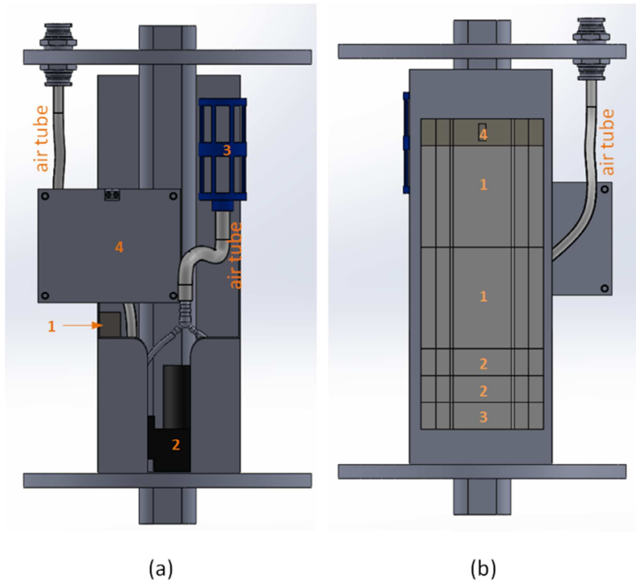

Figure 6. Internal construction of the control cabinet: (a) Layout of control layer: (1) Kuhnke proportional valve; (2) Miniature pump; (3) Silencer; (4) Amplifier circuit; (b) Layout of the power supply layer: (1) 12V-2A power supply unit; (2) 24V-1A power supply unit; (3) 5V-0.75A power supply unit; (4) circuit breaker.

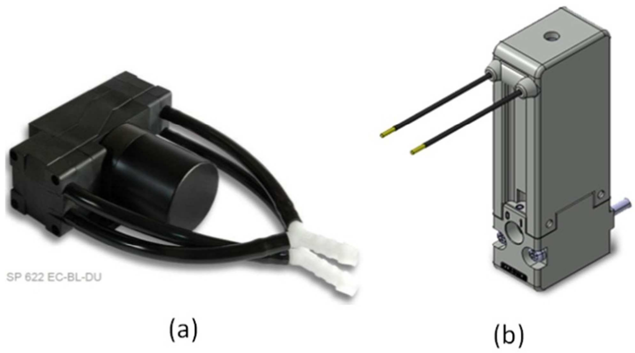

Figure 7. Miniature pump and proportion valve: (a) Pump SP 622 EC-BL-DU-DV produced by the company Schwarzer Precision in serial connection, which provides a maximal of 1.8 bar compressed air. (b) Kuhnke proportional valve Type 68P produced by the company Kendrion**.**

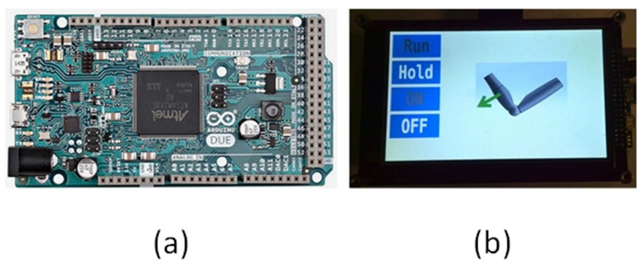

Figure 8. Control Core and touch control element: (a) Arduino Due board. This board consists of a 32-bit micro controller, a 512KB flash memory and a 92KB SRAM. (b) Control interface of the elbow trainer with four touch buttons, which can switch the device on and off as well as run and stop it. The image in the middle of the screen shows the current movement direction of the device.

3. Control System Conception

The general block diagram of the assistive control system is shown in Figure 9. In this control system, a simple PI controller is used. When combined with desired trajectory adaption, this control system does not need any pressure or force regulation and the influence of voluntary force from subjects can be considered by desired trajectory adaption. As shown in Figure 9, the PI controller generates the control voltages for the pump and valve of the integrated supply subsystem. The control voltages are generally defined as follows:

$$\vec{U} = [U_P \; U_V]^T, \qquad (4)$$

where U_P and U_V are the control voltages for pump and valve respectively. A rehabilitation robot usually uses external compressed air supply and servo valves. The supply system in this paper consists of a miniature pneumatic pump and a proportional valve as an air outlet valve, which is compact and can be integrated in rehabilitation devices. Additionally, the pump cannot produce large impact forces, which is beneficial for safe human-robot-interaction.

3.1. Control of the Pump

Unlike impedance control, the control voltages here are generated only with the position difference φ_e. U_P for the pump is calculated as follows:

$$U_P = \begin{cases} k_p\varphi_e + k_i \int \varphi_e \, dt \;\; if \; \varphi_e \in (0, \varphi_r] \\ 0 \; otherwise \end{cases}, \qquad (5)$$

where k_p and k_i are manually defined gain factors. A suitable value of k_p could be 0.03 and k_i could be settled around 0.002. The value of U_P only depends on the position difference φ_e. The part $k_p\varphi_e$ generates a voltage, which is proportional to the position difference. This part is usually not enough for a rehabilitation device to reach the final position, especially when the current position is very close to the final position and also when the position difference is very small. For this reason, the second part $k_i \int \varphi_e \, dt$ is used, which is proportional to the integral of position difference. The pump works only if the position difference φ_e in a positive safe range, which is defined from 0 to φ_r. The upper limit φ_r can be manually defined and a suitable value of φ_r can be between 20° and 30° for example.

In practical use, if there is not enough voluntary force from the subject, φ_e is then usually positive and the control voltage could be generated. A too large φ_e could cause a large force. For safety the pump should only work, if the value of φ_e is in the safe range, which can prevent the generation of a dangerous force on the subject caused by a too large position difference. Otherwise, if there is always enough voluntary force from the subject, φ_e could be zero or negative. In this case, no voltage will be generated.

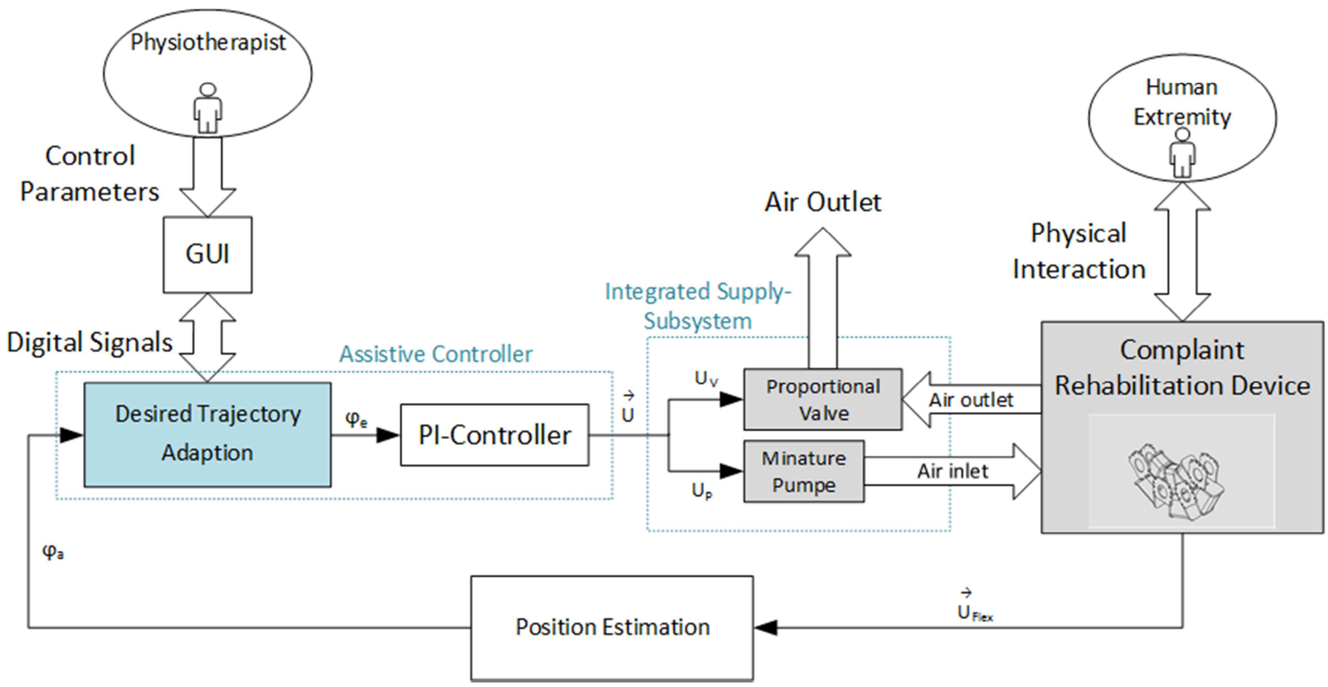

Figure 9. General block diagram: A general block diagram of an assistive control system for a pneumatic actuated complaint rehabilitation device. With this control system, a rehabilitation device provides safe interaction between a human and the device without using force or pressure regulation. All the needed control voltages are generated by a simple PI controller and combined with desired trajectory adaption. The assistive control is achieved only with position feedback.

3.2. Control of the Valve

The control voltage U_V for the air outlet valve depends also only on φ_e and it is calculated in a similar way as in the following:

$$U_V = \begin{cases} k_p\varphi_e + k_i \int \varphi_e\, dt + k_o \; if \; \varphi_e \in [\varphi_f, \varphi_s] \\ 0 \; otherwise \end{cases}, \tag{6}$$

The gain factors k_p and k_i are newly defined here and usually have different values as the gain factors by U_P. An offset voltage k_o is necessary for the proportional valve, which keeps the control voltage always in the work range of the valve. Its value depends only on the valve's properties. For this reason, k_o for different valves is usually set to different values and can only be determined manually through experiments.

The position estimation with flex sensor based on ANN, which was published in our previous work, is also used. The whole control system can be uploaded to a microcontroller and through the GUI on the touchscreen a physiotherapist can very easily control the system. But due to the performance of the microcontroller, the control parameter of the elbow trainer, as a demonstrate device, can now only be set and modified on the computer and subsequently uploaded to the microcontroller. The GUI presently does not support visualizing any input and output of state parameters.

4. Desired Trajectory Adaption

In order to achieve assistive control, a force or pressure regulation is usually needed. But as mentioned in the last section of this reported control algorithm, assistive control is achieved only by using position feedback and we call this algorithm *desired trajectory adaption*. The block diagram is shown in Figure 10. With this algorithm, we do not control the force or pressure but a time counter of desired trajectory. The influence of voluntary force from the subject is seen as an influence on the time counter and through time counter adaption, the control is assistive.

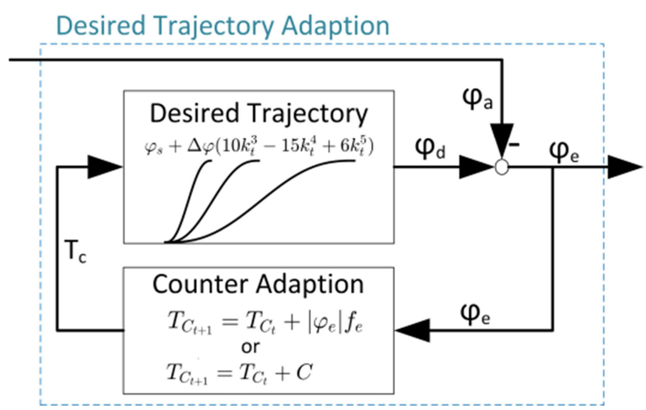

Figure 10. Desired Trajectory Adaption: The desired trajectory block defines basic movements of the robot, while the adaption law for time counter T_c is defined in the counter adaption block.

The desired trajectory adaption consists of two parts: the desired trajectory and the counter adaption, which are both shown in Figure 10. The basic desired trajectory is based on a Minimum-Jerk movement and each position on this trajectory is calculated as follows:

$$\varphi = \varphi_s + \Delta\varphi(10k_t^3 - 15k_t^4 + 6k_t^5), \tag{7}$$

where φ is a calculated position on desired trajectory, φ_s and φ_f are the start and final position respectively, $\Delta\varphi = \varphi_s - \varphi_f$ is the working range, $k_t = T_c/T_d$ is positive ratio between adaptive time counter T_c and the set run time T_d of the movement. If there is no voluntary force form the subject, this basic desired trajectory defines the movement of this robot and the robot moves periodically between initial and final position. If the current final position is reached, it is then assumed to be the next start position and the previous start position is assumed to be the next final position. The desired position φ_d at each point in time is calculated as follows:

$$\varphi_d = \begin{cases} \varphi_s + \Delta\varphi(10k_t^3 - 15k_t^4 + 6k_t^5) \; if \; k_t \in [0,1) \\ \varphi_f \; if \; k_t \in [1, \infty). \end{cases} \tag{8}$$

It is important to limit the desired position φ_d equal to the final position φ_f, if k_t is larger than 1. Because if k_t larger than 1, that means the counter T_c is larger than the set run time T_d and in this case the calculated position could be very large. Thus the position difference $\varphi_e = \varphi_d - \varphi_a$, where φ_a is the current position, could also be very large. This could generate a large control voltage for the pump, which may generate dangerous force for the subject. The equation 8 sets a limit for φ_d and keeps the force in a suitable range. The desired position will be compared with the current position and the difference φ_e will be sent to the PI controller and counter adaption block, respectively. In the counter adaption, an adaption law for time counter T_c is defined as follows:

$$T_{c_{t+1}} = \begin{cases} T_{c_t} + |\varphi_e| f_e \; if \; \varphi_e(\varphi_f - \varphi_s) < 0 \\ T_{c_t} + C \; sonst \end{cases}, \tag{9}$$

where $T_{c_{t+1}}$ is the value of the time counter T_c at the next time point, T_{c_t} is the current value of the time counter, f_e is a fitting constant and C is a constant step increment of the desired trajectory. When the position difference φ_e is negative, the counter at the next time point is assumed to be the sum of the current counter and an increment, which is proportional to $|\varphi_e|$ and f_e. This fitting constant f_e is manually chosen in this work and can be made adaptable to the movement speed in the later work. When the difference is positive, the increment of

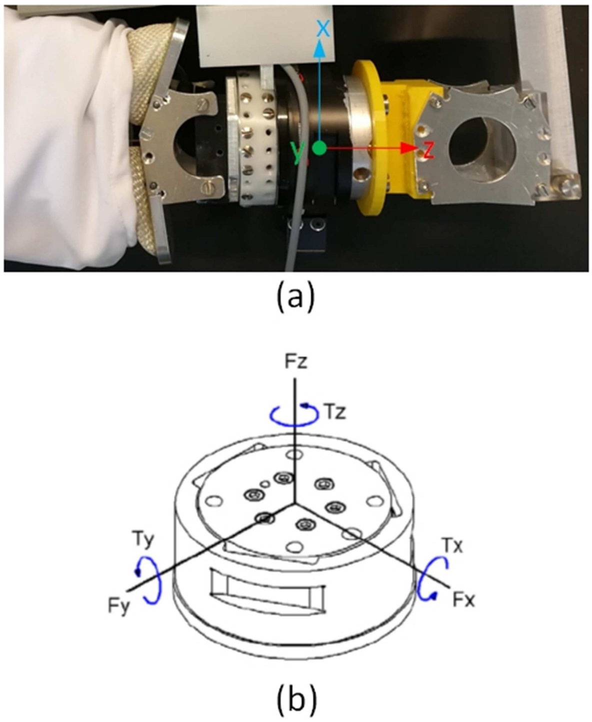

Figure 11. Force/Torque sensor installation: (a) additionally installed force/torque sensor to measure the performance curve and improve the assistive function of the robot; (b) the applied force and torque vector on a transducer.

the time counter will be a constant step increment C. Every time when the final position is reached and the current Minimum-Jerk movement is over, a new movement will be started and T_c will be reset to zero and will start to count the running time for a new movement afresh.

5. System Test Result

In order to measure the performance of the elbow trainer and to verify its function, an ATI Six-Axis Force/Torque Sensor FT7855 (ATI Industrial Automation, Apex, USA) has been installed on the elbow trainer. The Figure 11(a) shows how this transducer is mounted and Figure 11(b) shows the applied force and torque vectors on the transducer.

5.1. Performance Curve

In order to be informed about the performance of the elbow trainer specifically, the performance curve has to first be measured. An external air supply is used for this measurement, which can provide more than 3 bar of air pressure. The elbow trainer will firstly be driven under 1 bar air pressure. The actuator will be held, every 10°, from 10° to 60° and the corresponding force produced by actuator will be recorded. This process will be repeated from 1 bar to 3 bar at every 0.5 bar. The recorded value and polynomial fit is used to plot the performance curve. The Figure 12 shows the performance curve of the sREC actuator. The force, which was permanently directed parallel to the x-axis, is measured, because it is the main force, which drives this soft actuator. The force development is typical for soft actuators. This means, the closer the angle is to the final position, the smaller the force will be. To be noted are the remarkable force values developed at relatively small pressures.

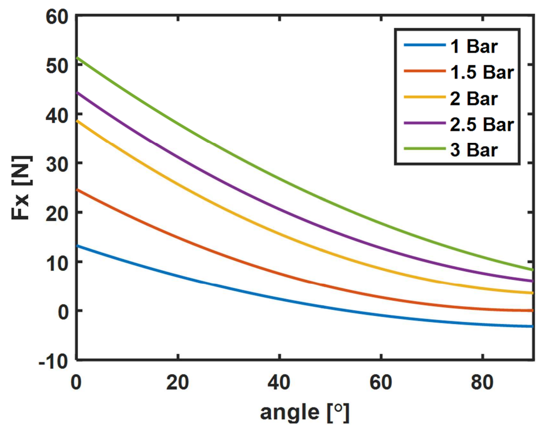

Figure 12. Performance curve of the elbow trainer under different pressure values.

5.2. Function Verification

The Figure 13 shows the result of the experiment on subject-A, which has a weight of 75 kg and a height of 179 cm. This experiment consists of three movement phases. The first two periods are called passive, the next two periods are called assistive-I and the last two periods are called assistive-II. During the passive phase the subject does nothing and the whole movement is accomplished by the robot alone. In the assistive-I and assistive-II phases, the subject may behave actively and use their own force and that of the robot together to accomplish the movement. In assistive-II phase, the voluntary force is larger than it is in assistive-I phase. In this test, the movement range is set from 5° to 60°.

The first plot shows the comparison between the desired position φ_d and current actual position φ_a. The second plot shows the pressure in the actuator. The third and fourth plot both show the force and torque vector measured by the transducer, respectively. As seen in the passive phase, there is a typical hysteresis between φ_d and φ_a and the pressure in the actuator reaches about 1.8 bar. The measured forces Fx and Fz, show the reaction forces, which are applied by the subject's arm on the actuator in the direction of the x-axis and the z-axis. The measured torque Ty is generated by these two reaction forces Fx and Fz and its absolute value is the torque generated by the actuator. There is also a torque on x-axis measured as a result of the force Fz. Analogous, a torque on z-axis is measured because of the force Fx.

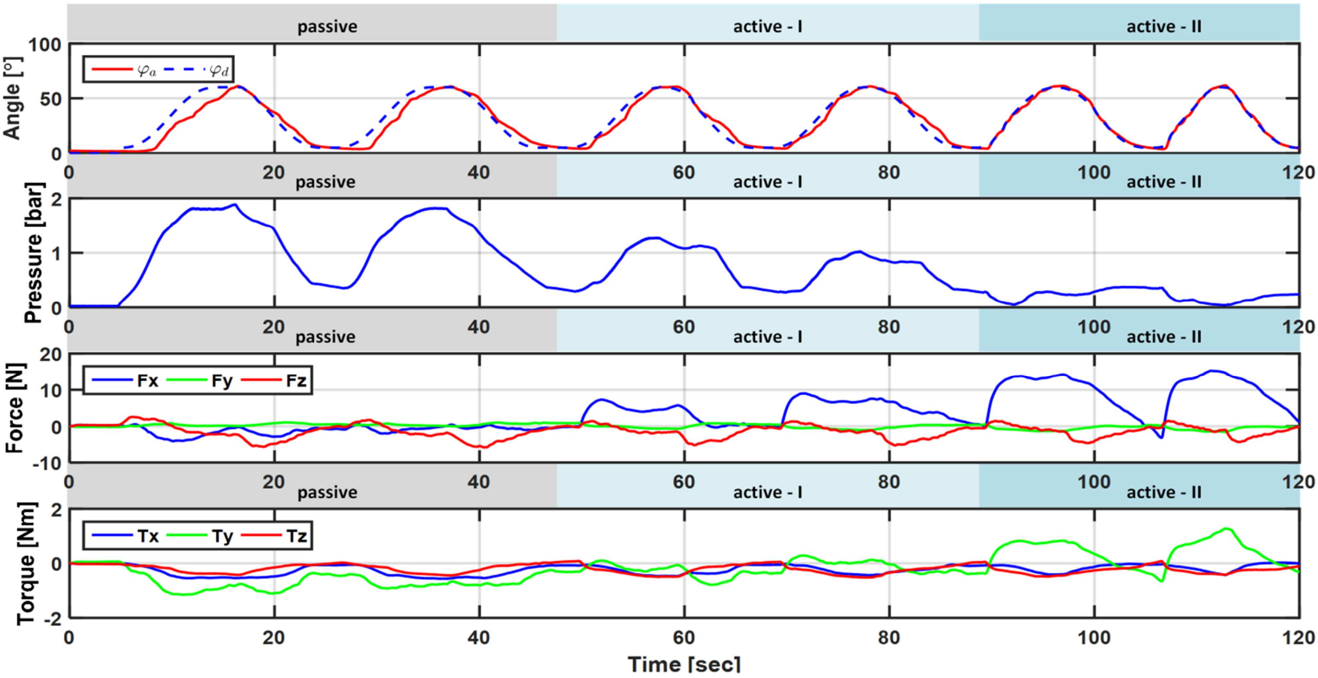

Figure 13. Test result of subject-A: In the passive phase, the subject tries to stay static and let the robot accomplish the movement on its own. The maximal pressure in the actuator is 1.8 Bar. The transducer measures the force and torque produced by the actuator. In the active I phase, the subject may move its arm with little force and the robot reduces its support, therefore the pressure in the actuator is less. The transducer measures the voluntary force and its torque. In active II, the subject enhances his voluntary force, which makes the robot to further reduce its support. The pressure is much less and the measured force is clearly higher.

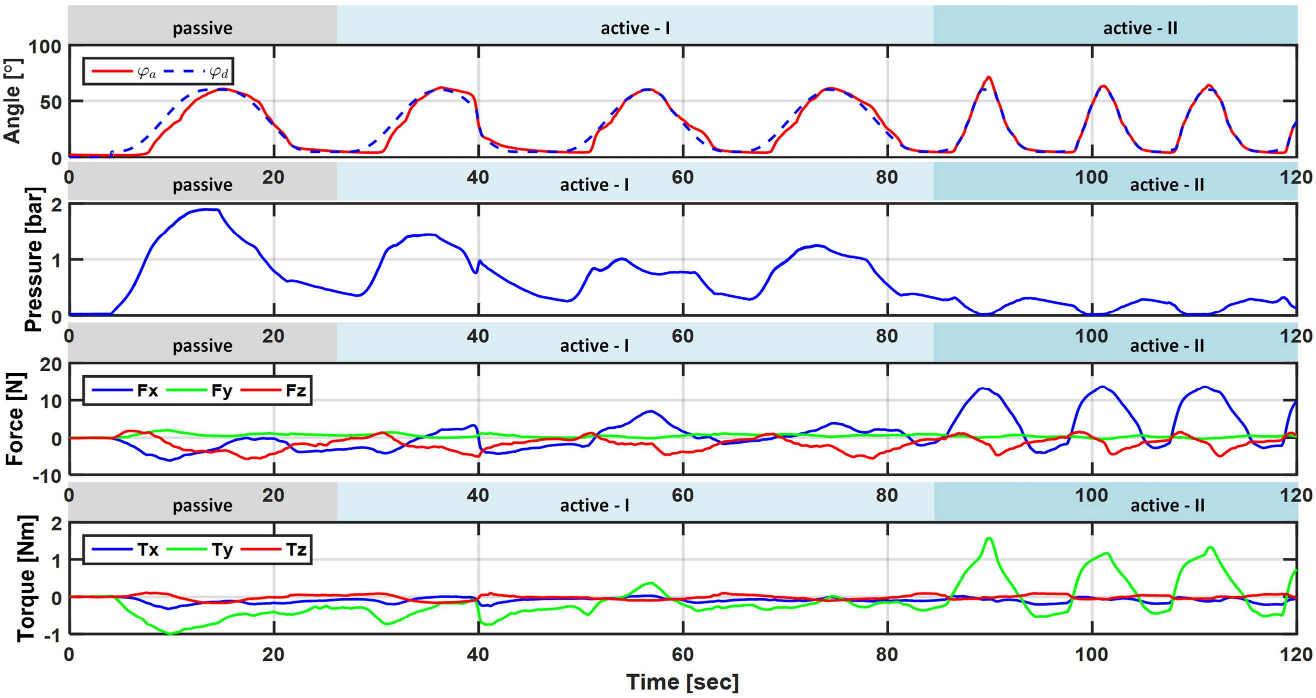

Figure 14. Test result of subject-B: If the subject cannot move his arm on its own, the robot applies the whole movement with enough support, as it is in the passive phase. If the subject can accomplish slight movement by itself, the robot reduces its support and encourages the subject to move by itself, as it is in the active-I phase. If the subject can apply movement totally on its own, the robot can further reduce its support even nearly up to zero, as it is in the active-II phase.

In the active-I phase, the hysteresis between φ_d and φ_a is smaller and φ_d and φ_a rise in a similar speed. The maximal pressure in this phase is about 1.2 bar, which is clearly smaller than it is in the passive phase. The Fx in this phase is no more a reaction force but a voluntary force from the subject. The measured maximum value of Fx is about 7.5N. In this phase the torque Ty is nearly about zero. This means, the torque generated by the weight of the arm is almost the same as the torque generated by the voluntary force. In the active-II phase, the hysteresis disappears. The desired trajectory is no longer a minimum-jerk-trajectory. The desired position φ_d adapts to the current position φ_a. The pressure is much less than it is in the active-I phase. The measured maximal voluntary force Fx is about 15N. The torque Ty is positive in this phase because the voluntary force is large enough to drive the actuator and the movement of the actuator is totally applied by the voluntary force. The air pressure in the actuator is inversely proportional to the voluntary force. This means that if the subject cannot carry out movement on its own, the robot gives enough support to help the subject move. If the subject carries out movement by itself, the robot gives less support and adapts to the subject's movement. The Figure 14 shows the experiment result of subject-B, which has a weight 91 kg and a height of 185 cm. Analogous, this result also consists of passive, active-I and active-II phases. In the passive phase, the subject is inactive. Because this subject has a larger weight, the measured torque Ty and force Fx are bigger compared to subject-A. In the active-I phase, the subject applies different higher voluntary forces. The voluntary force of the second period in this phase is visibly higher than it is in the other two periods. Therefore, the corresponding air pressure of this period is smaller. In the active-II phase, the voluntary force is much higher and the air pressure is much lower. This result also shows that this robot is capable of assistive support.

6. Conclusion

This paper presents a new algorithm for assistive control based on an integrated compressed air supply and desired trajectory adaption.

A commercially available miniature membrane pump without a buffer pressure tank is used. This makes the rehabilitation device much more compact, which therefore makes it also possible for ambulatory users to use rehabilitation devices at home. The noise produced by the pump can be intensely reduced by a normal cover box, so as to prevent noise pollution.

The reported assistive controller, which consists of a simple PI controller and desired trajectory adaption, does not use exact force or pressure regulation. In this controller the desired trajectory is not static, so it can adapt to the subject's active movement. This feature makes it possible to achieve assistive behavior using only position sensors, which simplifies the control system and reduces the device costs. The initially performed test confirms the interactive properties of the new controller. Compared to the assistive controller and the exact pressure regulator presented in [11], this controller provides its users more freedom of movement, even if their motion is less harmonic and seems to be better suitable for patients in the recovery process.

Next step is to make the control parameters adaptive to a patient's medical conditions which will make the system smarter and thereby increase the effectiveness of treatment while simultaneously reducing the physiotherapist's workload. Clinical assessments of devices with new assistive controllers are currently in an advanced project stage.

Acknowledgements

This work is partially supported by the German Federal Ministry of Education and Research (BMBF) through the cooperative research projects SE_BURG (grant 16SV6313) and inBURG (grant 13GW0152D). The authors appreciate the contribution from Dr.-Ing. André Wilkening in the development of the control concept during his time with FWBI.

References

[1] R. J. Sanchez, E. Wolbrecht, R. Smith, J. Liu, S. Rao, S. Cramer, T. Rahman, J. E. Bobrow und D. J. Reinkensmeyer, A Pneumatic Robot for Re-Training Arm Movement after Stroke:, in *9th IEEE International Conference on Rehabilitation Robotics (ICORR2005)*, Chicago, IL, USA, 2005.

[2] E. T. Wolbrecht, D. J. Reinkensmeyer und J. E. Bobrow, Pneumatic Control of Robots for Rehabilitation, *The International Journal of Robotics Research,* pp. 23-38, 2010.

[3] A. E. Jackson, R. J. Holt, P. R. Culmer, S. G. Makower, M. C. Levesley, R. C. Richardson, J. A. Cozens, M. M. Williams und B. B. Bhakta, Dual robot system for upper limb rehabilitation after stroke: the design process, *ARCHIVE Proceedings of the Institution of Mechanical Engineers Part C Journal of Mechanical,* Bd. 221, Nr. 7, 2007.

[4] P. R. Culmer, A. E. Jackson, S. G. Makower, R. C. Richardson, J. A. Cozens, M. C. Levesley und B. B. Bhakta, A Control Strategy for Upper Limb Robotic Rehabilitation With a Dual Robot System, *IEEE/ASME Transactions on Mechatronics,* Bd. 15, Nr. 4, 2010.

[5] S. Balasubramanian, R. W. a. M. Perez, B. Shepard, E. Koeneman, J. Koeneman und J. He, RUPERT: An Exoskeleton Robot for Assisting Rehabilitation of Arm Functions, in *Virtual Rehabilitation*, Canada, 2008.

[6] R. Morales, F. J. Badesa, N. García-Aracil, J. M. Sabater und C. Pérez-Vidal, Pneumatic robotic systems for upper limb rehabilitation, *Medical & Biological Engineering & Computing (MED BIOL ENG COMPUT),* Bd. 49, Nr. 3, pp. 1145-1156, 2011.

[7] S. Kousidou, N. Tsagarakis, D. Caldwell und C. Smith, Assistive Exoskeleton for Task Based Physiotherapy in 3-Dimensional Space, in *The First IEEE/RAS-EMBS International Conference on Biomedical Robotics and Biomechatronics*, Pisa, Italy, 2006.

[8] S. Kousidou, N. Tsagarakis, C. Smith und D. Caldwell, Task-Orientated Biofeedback System for the Rehabilitation of the Upper Limb, in *2007 IEEE 10th International Conference on Rehabilitation Robotics*, Noordwijk, Netherlands, 2007.

[9] T. G. Sugar, J. He, E. J. Koeneman, J. B. Koeneman, R. Herman, H. Huang, R. S. Schultz, D. E. Herring, J. Wanberg und Sivak, Design and Control of RUPERT: A Device for, *IEEE TRANSACTIONS ON NEURAL SYSTEMS AND REHABILITATION ENGINEERING,* Bd. 15, Nr. 3, 2007.

[10] A. Wilkening, D. Baiden und O. Ivlev, Assistive Acting Movement Therapy Devices with Pneumatic Rotary-Type Soft Actuators, *BMT - Biomedical Engineering,* Bd. 57, Nr. 6, pp. 445-456, 2012.

[11] A. Wilkening, H. Stoeppler und O. Ivlev, Adaptive Assistive Control of a Soft Elbow Trainer with Self-Alignment using Pneumatic Bending Joint, in *2015 IEEE International Conference on Rehabilitation Robotics (ICORR)*, Nanyang Technological University, Singapore, 2015.

[12] P. H. FWBI, Soft-Fluidic Actuator Elements and Processes for Their Manufacturing. Germany Patent DE102011081727, 2014.

[13] A. Wilkening, S. Hacker, H. Stöppler, L. Dürselen und O. Ivlev, Experimental and Simulation-based Investigation of Polycentric Motion of an Inherent Compliant Pneumatic Bending Actuator with Skewed Rotary Elastic Chambers, *Robotics,* Bd. 6, Nr. 2, 2017.

[14] Schwarzer-Precision, Schwarzer Precision 622 EC-BL-DU-DV, [Online]. Available: http://www.schwarzer.com/pdf/SP_PUMPS_DataSheet_ClassEC_Series600_Type620-622ECBLDU.pdf.

[15] Kendrion, Kuhke proportional valve, [Online]. Available: http://proportional-valves.kuhnke.kendrion.com/download/P813EN_Techn_Info_Kuhnke_Propventile.pdf.